

ARTICLE

OPEN

Capturing convection essential for projections of climate change in African dust emission

Luis Garcia-Carreras¹✉, John H. Marsham¹, Rachel A. Stratton³ and Simon Tucker³

The summertime Sahara and Sahel are the world's largest source of airborne mineral dust. Cold-pool outflows from moist convection ('haboobs') are a dominant source of summertime uplift but are essentially missing in global models, raising major questions on the reliability of climate projections of dust and dust impacts. Here we use convection-permitting simulations of pan-African climate change, which explicitly capture haboobs, to investigate whether this key limitation of global models affects projections. We show that explicit convection is key to capturing the observed summertime maximum of dust-generating winds, which is missed with parameterised convection. Despite this, future climate changes in dust-generating winds are more sensitive to the effects of explicit convection on the wider meteorology than they are to the haboobs themselves, with model differences in the change in dust-generating winds reaching 60% of current values. The results therefore show the importance of improving convection in climate models for dust projections.

npj Climate and Atmospheric Science (2021)4:44; <https://doi.org/10.1038/s41612-021-00201-x>

INTRODUCTION

Airborne mineral dust affects solar and infrared radiation^{1,2}, nucleates ice in clouds³, darkens snow and ice surfaces when deposited there⁴ and is a health hazard⁵. Dust deposited to the oceans and remote land can provide vital nutrients to the biosphere^{6,7}. Predicting dust on climate time scales is immensely challenging; an analysis of 23 global climate models used in the Fifth Assessment Report of the Intergovernmental Panel on Climate Change has shown that they fail to capture basic features of Earth's dust cycle and past inter-annual variability⁸. Such failures of dust models are due to a combination of the difficulty in representing the land surface^{9,10}, wet and dry deposition¹¹, the dust size distribution and radiative properties¹¹ and the rare high-wind events that dominate dust uplift^{12,13}.

For the Sahara and Sahel, dust uplift is dominated by the daytime breakdown of the nocturnal low-level jet (LLJ) as well as, in the summer, haboobs generated from convective storms. In the summer, when atmospheric dust loads reach their peak and convective activity is at its highest¹⁴, haboobs account for 50% of dust-generating winds in the southern Sahara¹⁵. Despite their importance as a dust uplift mechanisms, haboobs are almost entirely absent in models with parameterised convection¹⁶, which has been linked to systematic failures in dust forecasts¹⁷ and the inability of analyses to capture the summertime peak in dust-generating winds^{18–20}. The lack of haboobs in global climate models therefore fundamentally limits their ability to represent dust uplift and casts serious doubts on their ability to predict how dust emissions may change in the future.

Convection-permitting models, which are run at high enough resolution that the parameterisation of convection can be turned off, are able to resolve large storms and mesoscale convective systems with much more realistic organisation, as well as allowing the explicit development of downdraughts and cold pools^{21–23}. In addition to producing haboobs, the improved representation of convection in convection-permitting simulations has also been shown to generate a weaker Sahel–Sahara pressure gradient that

is more consistent with observations^{16,22,24}. This weakens LLJ uplift and demonstrates the potential impact of improved representation of convective storms beyond their direct impact via haboobs. While long-term biases in climate models often resemble average short-term errors in weather forecasts, until now it has been impossible to examine how the absence of haboobs affects climate change projections of dust emission. Here we use pan-African convection-permitting simulations of climate change^{25,26} to investigate how an explicit representation of convection and haboobs affects both modelled dust-generating winds and future climate changes in those winds.

Here we build on a previous study²⁵, which presented future climate projections of changes in extreme rain from 4.5 km grid-spacing regional simulations of African climate ('CP4'), alongside an equivalent 25 km run with parameterised convection ('P25'), to quantify the impact of explicitly capturing convection, and by association haboobs, on future climate changes in dust-generating winds. These simulations use 10 years of past climate (1997–2007, 'CP4' and 'P25'), and 10 years around 2100 under a Representative Concentration Pathway (RCP) 8.5 scenario ('CP4FC' and 'P25FC'). Observed sea surface temperatures (SSTs) in the current climate are modified by a spatially varying increment from the global parent model in the future run, to give two 10-year periods that can be compared. Model setups are detailed in Methods, but key to interpretation here is that the explicit convection improves the entire West African monsoon²⁶, as well as the intensity of storms within it²³.

RESULTS

Quantifying dust uplift potential and the influence of haboobs

Computational cost prevented use of prognostic dust in CP4 and P25, so we use the now widely used diagnostic, dust uplift potential (DUP)¹⁶, to analyse dust-generating winds. DUP is a necessary, but not sufficient condition for modelling dust. DUP is a threshold cubic function of wind speed, and therefore would

¹Department of Earth and Environmental Sciences, University of Manchester, Manchester, UK. ²School of Earth and Environment, University of Leeds, Leeds, UK. ³Met Office, FitzRoy Road, Exeter EX1 3PB, UK. ✉email: luis.garcia-carreras@manchester.ac.uk

control modelled dust uplift from a uniform bare land surface. In reality, uplift is affected by bare-soil fraction, soil moisture and soil type. Vegetation cover, which varies both spatially and seasonally across the region, not only affects uplift through changes in bare-soil fraction, but also impacts winds (and therefore DUP) through changes in surface roughness. The simulations include seasonally varying vegetation parameters and so the influence on winds of vegetation growth during the monsoon season is accounted for, but unvaried between the simulations. The use of DUP, however, allows dust-generating winds to be isolated, to allow understanding of the role of meteorology: real dust sources are localised and so any spatial shifts in patterns of DUP, as well as overall DUP changes are important.

Objectively identifying haboobs is extremely challenging^{24,27}, since ultimately any density current (e.g., a sea breeze) can have the same thermodynamic and dynamic characteristics as a haboob. Therefore, following previous studies, we rely on the distinctive seasonal cycle of haboobs and the clear difference in diurnal timing of LLJ and haboob events^{15,16,19,28}. We further support our findings by looking at high wind-speed events associated with precipitation, which are likely to be driven by haboobs²². Haboobs are much more common over the Sahara and Sahel in the summer when the West African monsoon provides moisture, contributing to the summertime peak in dust emissions that is found in observations. For this reason, the analysis focuses primarily on the summer months. LLJ wind events are caused by the breakdown of the nocturnal LLJ after sunrise, and therefore have a strong morning peak around 0900 local time^{15,28}. Haboobs, on the other hand, are present in the evening and night, as they are generated from storms that are triggered in the evening and persist overnight. We therefore use DUP at different times of day to isolate the impact of winds from the different sources. We confirm in our results analysis that morning DUP (dominated by the LLJ breakdown) is related to synoptic pressure gradients, whereas evening DUP (dominated by haboobs) is not: this is as expected from these two very different mechanisms for uplift, which supports our approach.

The Sahel and Sahara are vast and sparsely populated and there is a shortage of in situ data for model evaluation, and routine SYNOPs do not make observations at the correct times in the diurnal cycle to sample haboobs or LLJ effectively¹². We therefore focus our evaluation on sites where the AMMA¹² and Fennec field campaigns²⁹ have provided high time-frequency observations of near-surface winds (see ‘Methods’). AMMA stations are located in the Sahel, and Fennec stations in the Sahara, with the Bordj Badji Mokhtar (BBM) Fennec station in the south Sahara (Fig. 2a), close to the Saharan summertime dust maximum¹⁵.

Seasonal cycle in present-day DUP

Given the non-linear nature of DUP, differences in mean DUP can result from small differences in, for example, surface roughness of the model grid-square relative to the observation point, and so are not the most useful measure of model performance. Here we focus on the shape of the seasonal cycle, as it provides insights on how the processes driving dust-generating winds are represented in the model. Haboobs dominate Sahelian dust uplift in summer¹², have been shown to cause over 50% of uplift at BBM in June^{15,30}, but are much less significant further north¹⁹. Therefore only the Sahel (AMMA) and south Sahara (BBM) show a pronounced summertime DUP maximum in observations, when both LLJs and haboobs can drive dust uplift, with lower values during the rest of the year when haboobs are much rarer (Fig. 1c, e). This single annual maximum in summertime is captured by CP4, which can capture haboobs, but not in the P25 model where convection is parameterised. For example, in the Sahel stations P25 does have a summertime peak, but this is delayed relative to observations, and there is also a wintertime peak that is not found in the

observations. In the south Sahara there is no summertime peak in P25 at all, with relatively constant DUP from January to August. P25 does capture the autumn minimum in the Sahel and south Sahara, as this is associated with a minimum in the pressure gradient in this season³¹. These results suggest that the LLJ in P25 is too strong, compensating for the lack of haboobs in the Summer, but leading to an overestimation in Winter. In the central Sahara, which is further away from the region of active convection, the seasonal cycle is much weaker, reflecting a reduced importance of haboobs in dust uplift (Fig. 1e). Here, however, DUP in P25 is too high by about a factor of 3 compared to observations, consistent with too strong a LLJ. Tuning, which is commonly applied to dust models, could resolve the overall overprediction of winds in P25, but this could not resolve the large errors seen in its seasonal cycle.

To provide further evidence that the seasonal cycle errors in DUP found in the P25 simulation are caused by missing haboobs, we calculate the fraction of DUP that is associated with rainfall events (Fig. 1b, d, f), using the fact that rainfall above a certain threshold is likely to generate a downdraught, so strong wind speeds in the vicinity of rainfall events are therefore likely to be associated with the convection²². Here we attribute a wind event to rainfall if there is at least 1 mm h⁻¹ of precipitation within 1° of the wind event. Results were insensitive to the exact precipitation and distance thresholds used, having tested thresholds of 1–3 mm h⁻¹ and 1–3°, respectively (not shown).

The seasonal cycle in DUP in observations and CP4 is clearly driven by an increase in wind events associated with rainfall in the summer, with a very similar fraction of events in CP4 and observations linked to rainfall (Fig. 1b, d). This is not the case in P25. This is most apparent in the South Sahara (Fig. 1c, d) where <5% of DUP is associated with rainfall in P25, compared to >30% in both observations and CP4. In the Sahel (Fig. 1a, b), there is an increase in wind events near rainfall in the summer in P25. However, despite the overprediction of rainfall frequency in P25²⁵, it represents less than half the events relative to CP4 and observations in all months except August, and more importantly, it does not control the seasonal cycle in DUP in the same way. For example, even in the summer, the big increase in the fraction of DUP associated with rainfall increases much later (August) compared to the increase in total DUP (June–July). The role of haboobs is further revealed by considering the distribution of high wind-speed events: probability density functions of DUP in JJA show a similar distribution of wind events in both CP4 and P25 simulations, but only CP4 can reproduce the observed distribution of wind events linked to convection, supporting the conclusion that the differences in the seasonal cycle of DUP are linked to an improved representation of convectively driven events in CP4 (Supplementary Fig. 1).

Spatial differences in present-day summertime DUP

We now focus on the summer (JJA) period, when haboobs are most active, and make use of the distinctive diurnal cycles of haboobs and LLJs. P25 has higher DUP for 22–30N and, in the west, south of around 16N (brown colours in Fig. 2b), consistent with its deeper heat low (Supplementary Fig. 2) and stronger pressure gradients north and south of this (lines in Fig. 2b, and Supplementary Fig. 3). These local differences proportionately represent approximately 25–50% of the total local DUP, reaching as high as 100% (Fig. 2a and Supplementary Fig. 4). The enhanced DUP from 22–30N in P25 is similar in the morning (06–12 UTC; Fig. 2c) and afternoon/night (12–23 UTC; Fig. 2d), and matches differences in the pressure gradient (solid lines are associated with brown regions in Fig. 2c, d). This is because the pressure gradient provides a strong control on the mean wind speed in these areas throughout the day (Fig. 2e, f) and so on the intensity of the LLJ. In the south Sahara and Sahel; however, there is a reversal of the

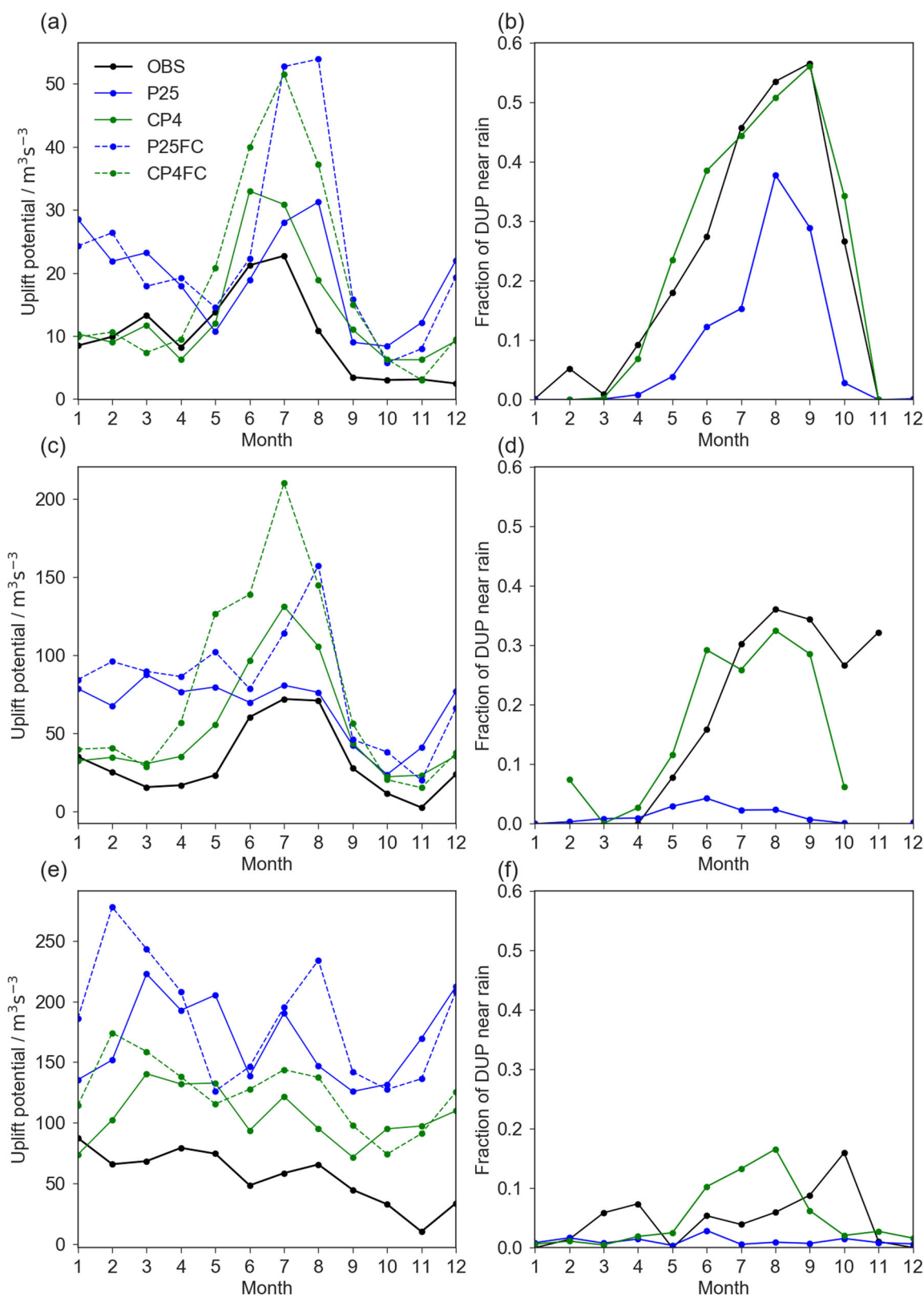


Fig. 1 Seasonal cycle of dust uplift potential (DUP). Total DUP at **a** Sahel stations, **c** South Sahara and **e** Saharan stations (plusses, circle and crosses in Fig. 2a, respectively) and fraction of the total monthly DUP that occurs near rainfall at **b** Sahel stations, **d** South Sahara and **f** Saharan stations.

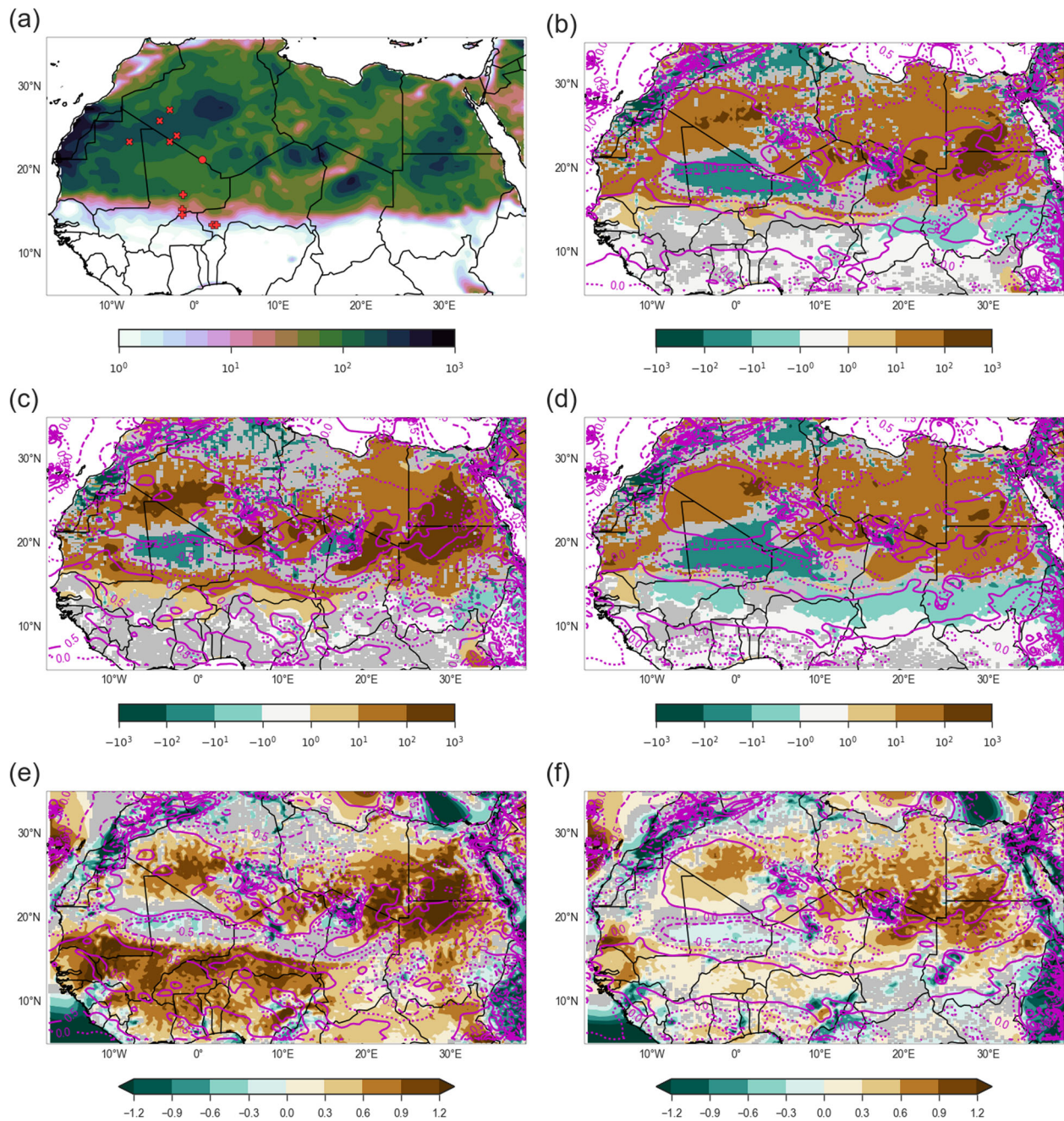


Fig. 2 Spatial differences in present-day summertime DUP. **a** JJA dust uplift potential ($\text{m}^3 \text{s}^{-3}$) in P25, **b-d** JJA dust uplift potential anomalies ($\text{m}^3 \text{s}^{-3}$, filled contours) and 925 mb geopotential height gradient anomalies (m, line contours) for P25-CP4: **b** all day average, **c** 0600–1200 UTC and **d** 1300–0300 UTC, **e, f** JJA mean wind speed anomalies (m s^{-1} , colours) and 925 mb geopotential height gradient anomalies (m, lines) for P25-CP4: **d** 0600–1200 UTC and **e** 1300–0300 UTC. Grey shading represents non-statistically significant differences at the 5% level. Red symbols in panel **a** show the locations of the ground stations shown in Fig. 1, where + symbols are the 'Sahel' stations (AMMA field campaign), x symbols are 'Sahara' stations and the circle is the 'South Sahara' station (Fennec field campaign).

signal between the morning and afternoon/night. CP4 has greater DUP in the afternoon/night when haboobs are active (green in Fig. 2d). This extends north into the areas around and downstream of the Hoggar and Air mountains ($\sim 5\text{--}10\text{E}$, $15\text{--}25\text{N}$), which are known areas for triggering of moist convection and haboobs. This high DUP in CP4 cannot be explained by the change in pressure gradient (line contours in Fig. 2d do not match the colours), or the change in mean wind (Fig. 2f), which all point to a haboob source. Conversely, P25 has greater DUP in this region in the morning, when its stronger pressure gradient gives stronger winds from the LLJ breakdown. We also note that CP4 also gives greater DUP over

the Bodele depression in northwest Chad (18E , 17N), greatest in the morning, indicating higher LLJ intensity as a result of the increased spatial resolution.

Future climate changes in DUP

Under climate change the low-level pressure increases in both runs, with larger increases in CP4 (Supplementary Fig. 2), but it increases least in the Sahara, i.e., there is a relative deepening of the SHL, as expected from previous studies³². In both models climate change leads to an increase in the DUP, except for the

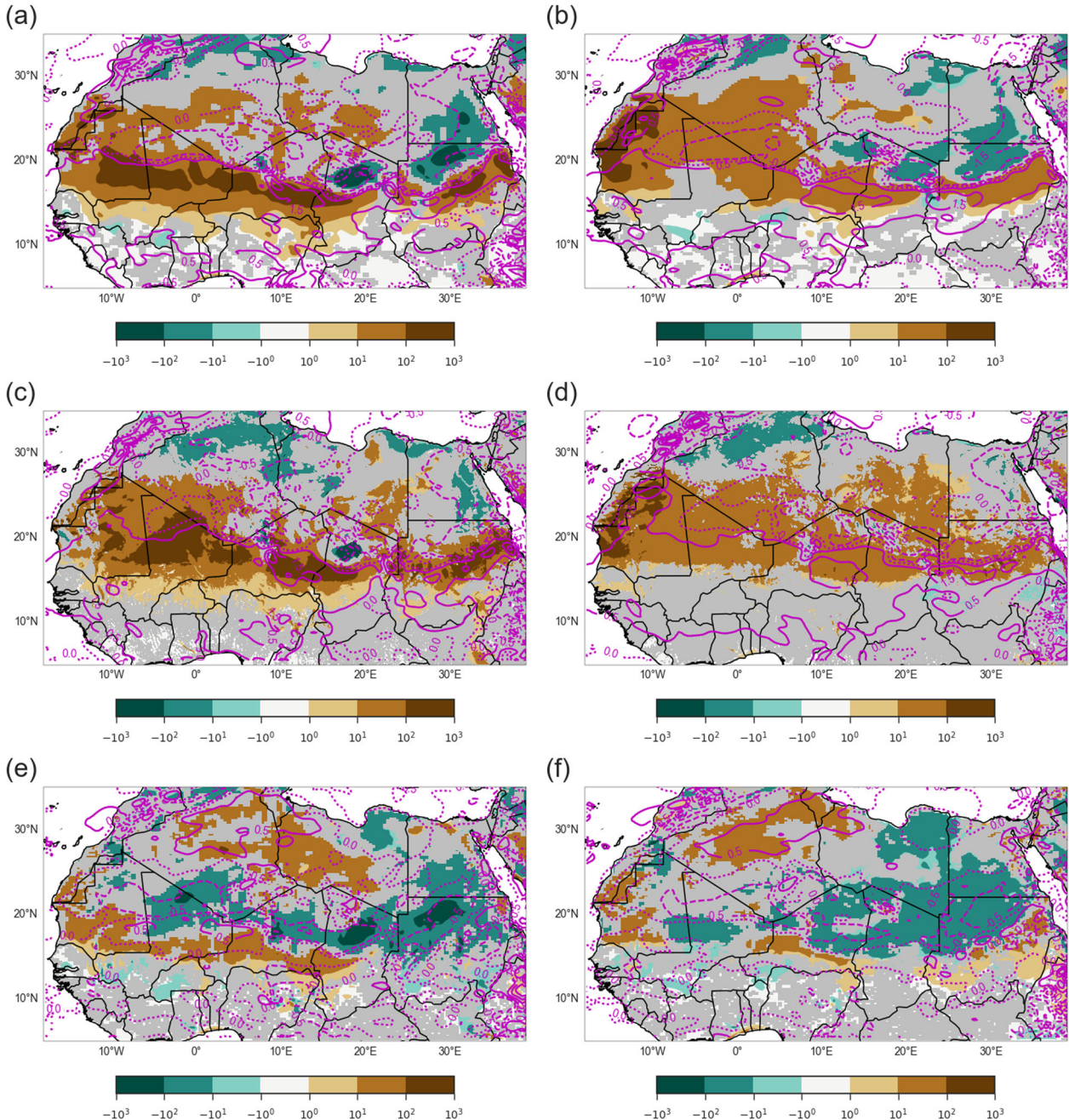


Fig. 3 Spatial differences in future climate changes in DUP. JJA dust uplift potential anomalies ($\text{m}^3 \text{s}^{-3}$, filled contours) and 925 mb geopotential height gradient anomalies (m, line contours) at **a, c, e** 0600–1200 UTC and **b, d, f** 1300–0300 UTC for **a, b** P25FC-P25, **c, d** CP4FC-CP4, **e, f** (P25FC-P25)-(CP4FC-CP4). Grey shading represents non-statistically significant differences at the 5% level.

most northern edge of the Sahara (Fig. 3a–d). The biggest increases occur in the morning along 20N, representing a relative increase of 25–50% compared to present-day values in both CP4 and P25 (Supplementary Fig. 5). These increases are aligned with increases in the gradient of the mean geopotential (Fig. 3a–d and Supplementary Fig. 6a–d) and are coincident with increases in mean wind speeds of $>0.8 \text{ m s}^{-1}$ (Supplementary Fig. 7). This is consistent with increased winds from the LLJ breakdown. Over the Bodele depression of Chad (18E, 17N), these changes are reversed, showing decreasing winds, DUP and pressure gradients, although these changes are weaker in CP4 (Fig. 3a, c). The similarity between colour and line contours shows that the largest changes in DUP from climate change, and differences between models are not a direct result of haboobs, but rather a result of the changing

pressure gradients, which are affected by the explicit convection in CP4.

Figure 3 does, however, reveal evidence of changing haboobs. In the evening there is a region where DUP does not increase in CP4's future climate between 0E–10E, south of ~18N, and also small decreases around 25E 12N (grey and green in Fig. 3d). The DUP changes here are much noisier than changes seen in the morning and coincide with a region of increased mean wind speeds (Supplementary Fig. 5d). The diurnal timing, noisy spatial pattern and lack of increase in DUP when mean wind and pressure gradient has increased all show that this is likely to be associated with compensating effects from decreased haboob uplift, consistent with reduced storm frequency also seen in these simulations²⁵. The total change in DUP here is dominated by the

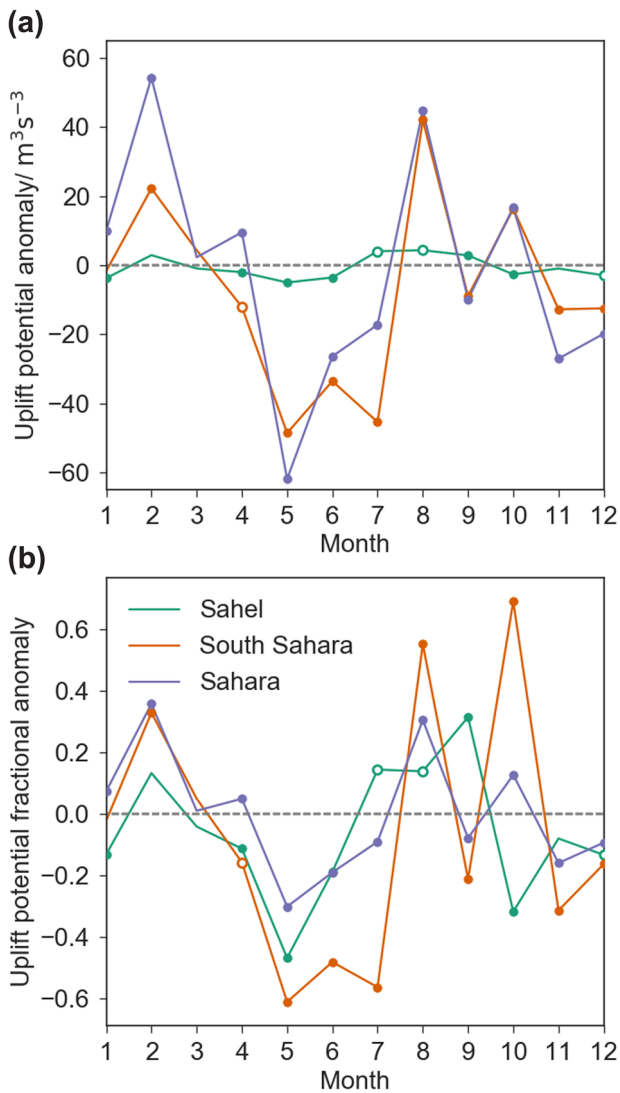


Fig. 4 Seasonal cycle in the forced change to DUP between P25 and CP4. **a** Absolute difference in the forced change to DUP: (P25FC-P25)–(CP4FC-CP4) and **b** difference in the forced change to DUP as a fraction of P25 current climate DUP: (P25FC-P25)–(CP4FC-CP4))/P25. Circles show statistically significant points at the 5% (filled) and 10% (hollow) level.

increased LLJ, however, and DUP in CP4 actually increases more here than in P25, giving a greater overall increase in CP4 in this key dust source region.

Again, considering the full annual cycle, Fig. 4 (see also dashed lines in Fig. 1) shows that the forced change in seasonal cycle varies significantly between the two models. Consistent with Fig. 3, P25 shows a much greater increase over the Sahel stations in summer, due to this model's strong LLJ increase, with little change in other seasons. In the south Sahara (BBM), both models have increased DUP in July and August, as the SHL deepens, but this increase develops earlier (from May) in CP4. Over the Fennec stations, the largest changes are increases in January, February and August, which are captured by both models, but generally the signal is not robust between the models (Fig. 4a). Differences between the climate change signals in P25 and CP4 are substantial, reaching 60% relative to the current climate DUP, with larger increases in CP4 in May–July (by 30–40%), and larger increases in P25 in August (30–60%, Fig. 4b).

DISCUSSION

In conclusion, convection-permitting simulations of pan-African climate change that are also able to capture the full annual cycle show that an explicit representation of convection is able to capture the seasonal cycle of dust-generating winds, whereas a parameterised simulation is not: the parameterised run misses the haboob-generated summertime peak in strong winds, which coincides with the observed summertime dust maximum. The dominant role of haboobs, which are missed by global models that all use parameterised convection, may explain much of their lack of skill for past climate⁸. Even though haboobs are maximised in summer, the mean spatial pattern in summertime climate change is broadly similar between the two runs: although the effect of changing haboobs has been identified, the bigger differences between the runs are caused by differences in their wider meteorology resulting from the change in convection, which substantially affects the future climate change in dust-generating winds. Explicit convection has large impacts on the seasonal cycle in climate change and overall the results highlight the importance of improving convection for dust in climate models and show that to produce well-founded predictions of summer dust and dust under climate change, models must include haboobs.

Parameterisations of haboobs have been developed that try and introduce the near-surface wind gusts associated with haboobs^{33–35}. Such a parameterisation does not change the diabatic heating and cooling from the model's convection parameterisation and so cannot capture the role of convection and haboobs in weakening the north–south pressure gradient, and therefore LLJs, in the way changing to an explicit representation of convection does. These results therefore show that deeper improvements to the entire representation of moist convection are expected to be most beneficial, due to the role of convection in affecting the wider meteorology. Such development of convection schemes is expected to take many years so haboob parameterisations will remain valuable in the shorter term. We note that, since capturing convection explicitly weakens the LLJ, if a haboob parameterisation is added to a model, it must be tuned to give the appropriate balance between haboobs and LLJs, rather than simply aiming to add haboob winds from an explicit run to a parameterised one.

METHOD

Models

The simulations used here all span the African continent and use the Met Office Unified Model (UM). Two model configurations are used: a 4.5-km resolution simulation (CP4), which is based on the UKV Met Office regional model used operationally in the UK since 2012, and a 25-km resolution simulation (P25), using a prototype version of the UM Global Atmosphere 7.0 (GA7) configuration. Both configurations use the same domain, land surface, aerosol forcings and are driven by boundary conditions derived by a global climate model with the same resolution and physical parameterisations as P25. Due to uncertainty in the land surface characteristics, uniform sandy soil is used over the Sahara in all the simulations. Aerosol concentrations are based on climatologies from 20-year climatological monthly means from past simulations³⁶ using the Coupled Large-Scale Aerosol Simulator for Studies in Climate interactive aerosols and dust scheme. A key difference between the two configurations is that in CP4 the parameterisation of convection is turned off, and a different cloud scheme and boundary layer scheme are used. The model configurations used for the present-day simulations have been described in more detail previously²⁶. Throughout the analysis the CP4 results were coarse-grained to the P25 grid, to allow a like-for-like comparison.

The present-day simulations span a 10-year period from March 1997 to February 2007 and are driven by SSTs from the Reynolds daily observations. The future climate simulations are driven by different SSTs, corresponding to a 10-year period around 2100, assuming an IPCC RCP 8.5 climate-change scenario. The key forcings used to simulate the future climate runs are perturbations to the SSTs; the climatological average SST

change between 1975 and 2005 and 2085–2115 in a HadGEM2-ES RCP8.5 run is added to the SSTs used in the present-day simulations. The future climate SSTs equate to a global mean increase of just under 4K relative to present day, which leads to a global mean 5.2K increase in 1.5 m temperature. The details of the future climate simulations have been described in detail previously²⁵.

Observations

Wind speed measurements are taken from ground stations in the Sahara and Sahel, covering different time periods (Fig. 2a). ‘Sahel’ stations (+ in Fig. 2a) are from the AMMA field campaign³⁷, and include two Atmospheric Radiation Measurement (ARM) Mobile Facilities (AMFs) at Niamey, Niger (2006) and three AMMA-CATCH stations in Agoufou (2005–2011), Bamba (2005–2010) and Koubou (2008–2010) located in Mali³⁸. Saharan stations are taken from the Fennec campaign. These include several automatic weather stations (AWSs) in remote Saharan regions (2011–2013, ‘x’ and ‘o’ in Fig. 2a)²⁹. To account for differences in time periods and avoid stations with more years dominating the means, we first compute mean seasonal cycles for each station individually, before averaging these to create the ‘Sahel’ and ‘Sahara’ seasonal cycles. The ‘South Sahara’ station at BBM is analysed separately as it is located far enough south that it has a particularly significant influence from convective storms and cold pools from the West African Monsoon¹⁵.

All AMMA stations reported 3 m wind speeds, while Fennec stations were at 2 m. In both cases the wind speeds had to be extrapolated up to 10 m for comparison with the model output. We adjusted the observed winds using the wind profile power law: $u = u_r \left(\frac{z}{z_r} \right)^\alpha$, where u_r is the observed wind at height z_r (2 or 3 m), z is the height to be adjusted to (10 m) and α is a stability coefficient. Here we use the same stability coefficients used previously with the same data¹⁹: 0.4 at night (1800–0600 UTC) and 0.2 during the day (0600–1800 UTC).

As several of the ground stations did not have rain gauges, we use precipitation data from the satellite-based Tropical Rainfall Measuring Mission product 3B42³⁹, which uses a combination of microwave data and calibrated infrared data. Data are available at 3 hourly and 0.25° temporal and spatial resolution.

Dust uplift potential

The paper uses DUP to represent dust-generating winds. DUP is threshold cubic function of wind speed, based on the wind component of a widely used parameterisations of dust uplift⁴⁰. It takes the form

$$\text{DUP} = U^3 \left(1 + \frac{U_t}{U} \right) \left(1 - \frac{U_t^2}{U^2} \right) \quad (1)$$

Where U is the wind speed, and U_t is a threshold wind speed, dependent on surface conditions. As in previous studies¹⁶ we use a constant threshold of 7 m s^{-1} , which is typical of the region⁴¹ and allows us to completely isolate the impact of dust-generating winds from changes in the land surface.

Statistical testing

A two-sided Welch’s *t*-test was used to test for statistical significance in differences between model runs (Figs. 2b–f and 3), using a 5% confidence level. Welch’s *t*-test was used as there is no assumption about the variance of the two samples being equal. The *t*-test requires that the distribution of means of samples taken from a population is normally distributed (but not necessarily the population distribution itself). Based on the Central Limit Theorem this will be the case if a sufficiently large number of samples are used. Even for extremely non-normal datasets, 500 samples are enough to fulfil this condition, a threshold that is passed in all our tests⁴².

DATA AVAILABILITY

The CP4 and P25 model datasets generated under the FCFA IMPALA project is publicly available on the Centre for Environmental Data Analysis (CEDA) archive. Saharan ground station data generated under the NERC funded Fennec project, and Sahel ground station data generated under the AMMA project are available on request from the authors.

CODE AVAILABILITY

Codes to produce the figures are available from the corresponding author.

Received: 7 August 2019; Accepted: 30 July 2021;

Published online: 24 September 2021

REFERENCES

- Haywood, J. M. et al. Can desert dust explain the outgoing longwave radiation anomaly over the Sahara during July 2003? *J. Geophys. Res. Atmospheres* **110**, D05105 (2005).
- Marsham, J. H. et al. The contrasting roles of water and dust in controlling daily variations in radiative heating of the summertime Saharan heat low. *Atmos. Chem. Phys.* **16**, 3563–3575 (2016).
- Niemand, M. et al. A particle-surface-area-based parameterization of immersion freezing on desert dust particles. *J. Atmos. Sci.* **69**, 3077–3092 (2012).
- Dang, C., Brandt, R. E. & Warren, S. G. Parameterizations for narrowband and broadband albedo of pure snow and snow containing mineral dust and black carbon. *J. Geophys. Res. Atmospheres* **120**, 5446–5468 (2015).
- Karanasiou, A. et al. Health effects from Sahara dust episodes in Europe: literature review and research gaps. *Environ. Int.* **47**, 107–114 (2012).
- Mahowald, N. M. et al. Atmospheric global dust cycle and iron inputs to the ocean. *Glob. Biogeochem. Cycles* **19**, GB4030 (2005).
- Jickells, T., Boyd, P. & Hunter, K. A. Biogeochemical impacts of dust on the global carbon cycle. In Knippertz, P., Stuut, J.-B.W. (Eds), *Mineral Dust: A Key Player in the Earth System* 359–384 (Springer Netherlands, 2014).
- Evan, A. T., Flamant, C., Fiedler, S. & Doherty, O. An analysis of aeolian dust in climate models. *Geophys. Res. Lett.* **41**, 2014GL060545 (2014).
- Cowie, S. M., Knippertz, P. & Marsham, J. H. Are vegetation-related roughness changes the cause of the recent decrease in dust emission from the Sahel? *Geophys. Res. Lett.* **40**, 1868–1872 (2013).
- Zender, C. S. & Kwon, E. Y. Regional contrasts in dust emission responses to climate. *J. Geophys. Res. Atmospheres* **110**, D13201 (2005).
- Huneeus, N. et al. Global dust model intercomparison in AeroCom phase I. *Atmos. Chem. Phys.* **11**, 7781–7816 (2011).
- Bergametti, G. et al. Dust uplift potential in the Central Sahel: an analysis based on 10 years of meteorological measurements at high temporal resolution. *J. Geophys. Res. Atmospheres* **122**, 12,433–12,448 (2017).
- Cowie, S. M., Marsham, J. H. & Knippertz, P. The importance of rare, high-wind events for dust uplift in northern Africa. *Geophys. Res. Lett.* **42**, 8208–8215 (2015).
- Marsham, J. H., Parker, D. J., Grams, C. M., Taylor, C. M. & Haywood, J. M. Uplift of Saharan dust south of the intertropical discontinuity. *J. Geophys. Res. Atmospheres* **113**, D21102 (2008).
- Marsham, J. H. et al. Meteorology and dust in the central Sahara: observations from Fennec supersite-1 during the June 2011 Intensive Observation Period. *J. Geophys. Res. Atmospheres* **118**, 4069–4089 (2013).
- Marsham, J. H., Knippertz, P., Dixon, N. S., Parker, D. J. & Lister, G. M. S. The importance of the representation of deep convection for modeled dust-generating winds over West Africa during summer. *Geophys. Res. Lett.* **38**, L16803 (2011).
- Pope, R. J., Marsham, J. H., Knippertz, P., Brooks, M. E. & Roberts, A. J. Identifying errors in dust models from data assimilation. *Geophys. Res. Lett.* **43**, 9270–9279 (2016).
- Largeray, Y. et al. Can we use surface wind fields from meteorological reanalyses for Sahelian dust emission simulations? *Geophys. Res. Lett.* **42**, 2490–2499 (2015).
- Roberts, A. J. et al. New Saharan wind observations reveal substantial biases in analysed dust-generating winds. *Atmos. Sci. Lett.* **18**, 366–372 (2017).
- Trzciak, T. M., Garcia-Carreras, L. & Marsham, J. H. Cross-Saharan transport of water vapor via recycled cold pool outflows from moist convection. *Geophys. Res. Lett.* **44**, 1554–1563 (2017).
- Bryan, G. H. & Morrison, H. Sensitivity of a simulated squall line to horizontal resolution and parameterization of microphysics. *Mon. Weather Rev.* **140**, 202–225 (2011).
- Roberts, A. J. et al. Can explicit convection improve modelled dust in summertime West Africa? *Atmos. Chem. Phys.* **18**, 9025–9048 (2018).
- Crook, J. et al. Assessment of the representation of West African storm lifecycles in convection-permitting simulations. *Earth Space Sci.* **6**, 818–835 (2019).
- Heinold, B. et al. The role of deep convection and nocturnal low-level jets for dust emission in summertime West Africa: estimates from convection-permitting simulations. *J. Geophys. Res. Atmos.* **118**, 4385–4400 (2013).
- Kendon, E. J. et al. Enhanced future changes in wet and dry extremes over Africa at convection-permitting scale. *Nat. Commun.* **10**, 1794 (2019).
- Stratton, R. A. et al. A Pan-African convection-permitting regional climate simulation with the Met Office Unified Model: CP4-Africa. *J. Clim.* **31**, 3485–3508 (2018).

27. Chaboureau, J.-P. et al. Fennec dust forecast intercomparison over the Sahara in June 2011. *Atmos. Chem. Phys.* **16**, 6977–6995 (2016).
28. Allen, C. J. T. & Washington, R. The low-level jet dust emission mechanism in the central Sahara: observations from Bordj-Badji Mokhtar during the June 2011 Fennec Intensive Observation Period. *J. Geophys. Res. Atmospheres* **119**, 2990–3015 (2014).
29. Hobby, M. et al. The Fennec Automatic Weather Station (AWS) Network: monitoring the Saharan climate system. *J. Atmos. Ocean. Technol.* **30**, 709–724 (2013).
30. Allen, C. J. T., Washington, R. & Engelstaedter, S. Dust emission and transport mechanisms in the central Sahara: Fennec ground-based observations from Bordj Badji Mokhtar, June 2011. *J. Geophys. Res. Atmospheres* **118**, 6212–6232 (2013).
31. Knippertz, P. Dust emissions in the West African heat trough: the role of the diurnal cycle and of extratropical disturbances. *Meteorol. Z.* **17**, 553–563 (2008).
32. Dong, B. & Sutton, R. Dominant role of greenhouse-gas forcing in the recovery of Sahel rainfall. *Nat. Clim. Change* **5**, 757–760 (2015).
33. Pantillon, F., Knippertz, P., Marsham, J. H., Panitz, H.-J. & Bischoff-Gauss, I. Modeling haboob dust storms in large-scale weather and climate models. *J. Geophys. Res. Atmospheres* **121**, 2090–2109 (2016).
34. Pantillon, F., Knippertz, P., Marsham, J. H. & Birch, C. E. A parameterization of convective dust storms for models with mass-flux convection schemes. *J. Atmos. Sci.* **72**, 2545–2561 (2015).
35. Nakamura, K., Kershaw, R. & Gait, N. Prediction of near-surface gusts generated by deep convection. *Meteorol. Appl.* **3**, 157–167 (1996).
36. Walters, D. et al. The Met Office Unified Model Global Atmosphere 6.0/6.1 and JULES Global Land 6.0/6.1 configurations. *Geosci. Model Dev.* **10**, 1487–1520 (2017).
37. Lebel, T. et al. The AMMA field campaigns: multiscale and multidisciplinary observations in the West African region. *Q. J. R. Meteorol. Soc.* **136**, 8–33 (2010).
38. Lebel, T. et al. AMMA-CATCH studies in the Sahelian region of West-Africa: an overview. *J. Hydrol.* **375**, 3–13 (2009).
39. Huffman, G. J. et al. The TRMM Multisatellite Precipitation Analysis (TMPA): quasi-global, multiyear, combined-sensor precipitation estimates at fine scales. *J. Hydrometeorol.* **8**, 38–55 (2007).
40. Marticorena, B. & Bergametti, G. Modeling the atmospheric dust cycle: 1. Design of a soil-derived dust emission scheme. *J. Geophys. Res. Atmospheres* **100**, 16415–16430 (1995).
41. Chomette, O., Legrand, M. & Marticorena, B. Determination of the wind speed threshold for the emission of desert dust using satellite remote sensing in the thermal infrared. *J. Geophys. Res. Atmospheres* **104**, 31207–31215 (1999).
42. Lumley, T., Diehr, P., Emerson, S. & Chen, L. The importance of the normality assumption in large public health data sets. *Annu. Rev. Public Health* **23**, 151–169 (2002).

ACKNOWLEDGEMENTS

All authors were funded by the NERC/DFID Future Climate for Africa IMPALA project (NE/M017176/1), with J. H. M. also funded by AMMA2050 (NE/M020126/1), SWAMMA (NE/L005352/1) and NCAS ACREW. The Fennec AWS network was developed, tested

and installed as part of Fennec project (NE/G017166/1). AMMA-CATCH system was funded by the French Ministry of Research and National Institute for Earth Sciences and Astronomy. Data from two AMF sites are provided by ARM Climate Research Facility.

AUTHOR CONTRIBUTIONS

L. G.-C. carried out the analysis and wrote the paper. J. H. M. advised on the analysis and contributed extensively to the paper. R. A. S. carried out the CP4 and P25 present-day experiments and S. T. carried out the equivalent experiments for future climate. All authors commented on the paper.

COMPETING INTERESTS

The authors declare no competing interests.

ADDITIONAL INFORMATION

Supplementary information The online version contains supplementary material available at <https://doi.org/10.1038/s41612-021-00201-x>.

Correspondence and requests for materials should be addressed to Luis Garcia-Carreras.

Reprints and permission information is available at <http://www.nature.com/reprints>

Publisher's note Springer Nature remains neutral with regard to jurisdictional claims in published maps and institutional affiliations.



Open Access This article is licensed under a Creative Commons Attribution 4.0 International License, which permits use, sharing, adaptation, distribution and reproduction in any medium or format, as long as you give appropriate credit to the original author(s) and the source, provide a link to the Creative Commons license, and indicate if changes were made. The images or other third party material in this article are included in the article's Creative Commons license, unless indicated otherwise in a credit line to the material. If material is not included in the article's Creative Commons license and your intended use is not permitted by statutory regulation or exceeds the permitted use, you will need to obtain permission directly from the copyright holder. To view a copy of this license, visit <http://creativecommons.org/licenses/by/4.0/>.

© The Author(s) 2021